Ag-zeolites as fungicidal material: Control of citrus green mold caused by *Penicillium digitatum*

J.L. Cerrillo[a], A.E. Palomares[a]*, F. Rey[a], S. Valencia[a], L. Palou[b], M.B. Pérez-Gago[b]

[a]*Instituto de Tecnología Química (CSIC-Universitat Politècnica de València), Camino de Vera s/n, 46022 Valencia, Spain.*

[b]*Instituto Valenciano de Investigaciones Agrarias IVIA, C. de Tecnología Poscosecha (CTP), Ctra. CV-315 km 10.7, 46113 Moncada, Spain.*

* Corresponding author:
Antonio Eduardo Palomares
E-mail address: apalomar@iqn.upv.es
Instituto de Tecnología Química, UPV-CSIC,
Universitat Politècnica de València
Camino de Vera s.n.46022 Valencia (Spain)
(+34) 96 387 7007 (ext. 76377)

Abstract

One of the most economically important postharvest diseases of citrus fruit is green mold caused by the fungus *Penicillium digitatum*. In this investigation, the antifungal properties of silver FAU and silver LTA zeolites against *P. digitatum* either alone or incorporated into edible coatings were evaluated in citrus fruit. The Ag-zeolites were characterized by different techniques such as ICP, TPR, XRD and electronic microscopy. These techniques demonstrated that ion exchange was a suitable method for the incorporation of silver cations into zeolites without changing the structure of the matrix. It was observed that silver was present in the zeolite mainly as well dispersed Ag^+ and that different silver species with different reduction properties were formed depending on the zeolite structure. It was found that the resulting materials had potential to control citrus green mold caused by *P. digitatum*. The results confirmed that incorporation of these zeolites into edible coatings provided an affordable and safe method to control decay of fresh oranges. The antifungal activity depended on the amount of silver contained in zeolites, but a high silver content induced phytotoxicity in the fruit surface. Nevertheless, Ag-zeolites with low silver content were also active without phytotoxic effects. The best results were obtained with the FAU zeolite, which had the largest pores and the highest Si/Al, showing the influence of the topology and composition of the zeolites on their antifungal properties.

Keywords

Silver, zeolites, edible coatings, antifungal properties, *P. digitatum*

1. Introduction

FAO reports [1] have shown that the third part of the food produced in the world goes to waste. This means that 100 Kg/year&person and 680 billion dollars are thrown away in industrialized countries. Fruits, vegetables, roots and tuber have the highest rates of waste, which has been estimated around 45%, and the main part of this waste is produced from harvest to market. Physiological and biochemical changes in the commodities, as well as possible physical injuries at harvest and during prolonged storage, can favor the development of pathogens causing disease, which are one of the most important causes of losses through the supply chain [2].

One of the most economically important pathogen that infects the fruit through rind wounds or injuries is the fungus *Penicillium digitatum* (Pers.:Fr.) Sacc., which causes green mold in citrus fruit. For many years, synthetic fungicides have been employed to control this disease. However, intensive and prolonged use of these chemicals have raised consumer concerns about human health risks and environmental pollution, being necessary the development of safer alternatives [3]. Several metal cations such as Ag^{+}, Zn^{++} or Cu^{+} have received a lot of attention as potential antimicrobial agents. Among them, silver is an interesting option due to the broad spectrum of its antimicrobial properties. In fact, silver compounds have been used as antibacterial agents since the ancient Greek and nowadays they are used as additives in bandages, socks, water filters and in new materials with biocide properties [4-6]. Recently, it has been proposed the use of silver in the food industry as antimicrobial packaging ingredient expected to provide affordable and safe food packaging solutions to increase food shelf-life [7, 8].

Silver can be easily incorporated into different carrier support materials such as polymers, metal oxides, clays or zeolites [9]. These materials behave as silver reservoirs, increasing the shelf-life and safety of treated food products. It has been described that the antibacterial activity of different Ag-containing materials depended on the chemical and structural characteristics of the compounds. For instance, Lalueza *et al*. [4] reported a different biocide effect for different silver-containing materials. These results indicated that the biocide activity of the materials was related to the total amount of ionic silver bioavailable, the oxidation state of the silver species and its particle size. In general, it has been described [10] that smaller silver particles had higher antimicrobial capacity, but these particles tended to aggregate leading to a reduction of the biocide properties. This can be avoided with the use of silver zeolites prepared by ion exchange [11]. In general, for food

applications, zeolites are among the most widely used materials to incorporate silver as antimicrobial agent. In the USA, zeolite-based technologies are listed under the US FDA Inventory of Effective Food Contact Substance Notifications for use in food-contact polymers [12]. In Europe, the EFSA also released a positive opinion concerning the use of two zeolites containing Ag ions in food contact surfaces, with silver migration into food matrices being restricted to 50 μg Ag of food [13]. In recent years, different zeolites containing Ag, Cu or Zn have been applied for antibacterial purposes [4, 9, 12-25]. Thus, Ferreira *et al* [9] studied the antimicrobial potential of silver faujasite against different bacteria (*Escherichia coli* and *Bacillus subtilis*) and yeasts (*Saccharomyces cerevisiae and Candida albicans*). They showed that the antimicrobial properties were generated by the silver present in the zeolite structure, obtaining better results with AgY than with AgX. Laluleza *et al* [26] studied the use of Ag-MFI at low Ag loadings against *Staphylococcus aureus*, noticing a correlation between the bactericidal efficiency and the Ag^+ released.

There are not many papers studying the use of silver zeolites as fungicide materials and only the antifungal properties of silver exchanged A zeolite [27], silver mordenite [10] and silver faujasite [9] have been described. In these works, silver A zeolite was effective against *Aureobasidium pullulans* fungus, silver mordenite against *Rhizopus oryzae*, *Mucor circinelloides* and *Geotrichum candidum*, and silver faujasite against *C. albicans, Pycnoporus cinnabarinus* and *Pleurotus ostreatus*. However, to our knowledge, no studies about the use of silver zeolites against *P. digitatum* have been published. The current investigation evaluates the use of two different silver zeolites as postharvest antifungal treatments against *P. digitatum* either alone or incorporated into edible coatings for citrus fruit, specifically oranges. The development of composite natural edible coatings to substitute conventional citrus waxes or the incorporation of low-toxicity antifungal ingredients to replace the use of synthetic fungicides are currently active research fields [3]. Besides acting as a support matrix for the active antifungal ingredient, these edible coatings applied to the fruit surface create a barrier to water vapor and oxygen that will help to control weight loss and respiration rate [28].

2. Experimental

2.1. Preparation of Ag-zeolites

A Na-FAU zeolite and a Na-LTA zeolite have been used as parent zeolites. FAU is a large pore zeolite and LTA is a small pore one, both of them containing large cavities. FAU zeolite was supplied by Zeolyst (CBV100) and LTA from Sigma-Aldrich (4A). The parent Na-zeolites were ion exchanged using $AgNO_3$ solutions at different concentrations in order to obtain a FAU zeolite and a

LTA zeolite in which Na^+ was completely exchanged by Ag^+ (total exchange, te) and zeolites with around 1-2% wt of silver (partial exchange, pe). The ion exchange procedure was performed with a solid/liquid ratio of 1/100 at 25 ºC for 16 h, under mechanical stirring and in darkness to avoid reduction of Ag^+ to Ag^0 [29]. Then, solids were filtered in darkness and washed to remove excess of silver solution; afterwards, the zeolite was dried at 100 ºC for 24 h and stored in darkness before application. Prepared samples and their compositions are summarized in Table 1.

2.2. Characterization

The chemical composition of the samples was measured by inductively coupled plasma (ICP-OES) in a Varian 715-ES ICP-Optical Emission Spectrometer. Prior to analysis, 30 mg of each sample were digested with concentrated nitric acid and concentrated hydrofluoric acid for 24 h. Afterwards, solutions were analysed by ICP-OES.

Scanning electron microscopy (SEM) images were obtained with a JEOL JSM-6300 LINK. This microscope has an energy dispersive X-ray equipment (EDX) system for semi-quantitative analysis and mapping of elements that was used to quantify and to evaluate the distribution of the elements in the zeolites. Samples were coated with graphite and X-ray spectra were obtained with an accelerating voltage of 20 kV.

A Philips X'Pert (Cubix)-advance diffractometer coupled to a copper anode X-ray tube was used for the X-ray diffraction (XRD) characterization. Compounds were conventionally identified using the JCPDS files.

Temperature-programmed reduction studies with H_2 (H_2-TPR) were carried out with a TPD-TPR Autochem 2910 equipment using a thermal conductivity detector (TCD). Samples were treated under Ar flow during 30 min and then the gas-flow was changed to a mix of 10% H_2 in Ar and the temperature was increased from room temperature up to 850 ºC with a ramp of 10 ºC/min.

2.3. Antifungal tests

Oranges (*Citrus sinensis* (L.) Osbeck) cv. 'Valencia' were artificially inoculated with *P. digitatum* (inoculum density of 10^5 spores/mL) by immersing a stainless steel rod with a probe tip of 1 mm wide and 2 mm in length into the spore suspension and wounding the rind of each fruit in one point at the equator. The Ag-zeolites were dispersed in water or incorporated into a hydroxypropyl methylcellulose (HPMC)-lipid composite edible coating at different concentrations. For coating formulation, emulsions were prepared by combining the HPMC (1.2% wet basis, wb), beeswax (BW; 3.5% wb) and Ag-zeolites (1.0 or 2.0% wb) suspended in water. Glycerol and stearic

acid were used as plasticizer and emulsifier, respectively. Ratios of HPMC-glycerol and BW-stearic acid were 2:1 and 5:1 (dry basis, db), respectively. Emulsions were prepared as described previously by Valencia-Chamorro et al. [30].

Preliminary screenings were conducted by placing 30 μL of the corresponding zeolite aqueous suspension in the rind wound about 24 h after fungal inoculation in order to assess the curative activity of the treatments. Coatings amended with Ag-zeolites were also applied as drops in the wounds or covering the entire fruit 24 h after fungal inoculation. Inoculated but untreated fruit were used as controls. Disease incidence (% of infected fruit) and severity (lesion diameter), pathogen sporulation (%) and visible phytotoxicities in the fruit rind were determined after 7 days of incubation at 20 ºC and 90% relative humidity. In every experiment, treatments were applied to 3 replicates of 10 fruit each.

3. Results and discussion

3.1. Characterization of Ag-zeolites

Table 1 shows the chemical composition and the level of silver ion exchange in the different zeolites studied in this work, FAU and LTA with different Si/Al ratio. Both zeolites were partially silver ion exchanged (pe) in order to obtain two samples with a similar silver content (1-2 wt %). Besides, other two samples were prepared to obtain FAU zeolite and LTA zeolite with an almost total silver ion exchange (te). Although the ion exchange procedure followed to incorporate the silver into both zeolites was similar (same precursor, same contact time, same temperature and same liquid/solid ratio), zeolites with different silver content were obtained after complete ion exchange, due to the fact that FAU and LTA zeolites have different Si/Al ratio. Hence, complete ion exchange in the LTA zeolite (Si/Al ratio = 1) resulted in 48% wt silver content in the zeolite whilst complete ion exchange in the FAU zeolite (Si/Al = 2.5) resulted in 31% wt silver content. On the other hand, a different ion exchange percentage is obtained when a fixed quantity of silver is introduced in zeolites with different Si/Al ratios.

As shown in Table 1, similar results in terms of the amount of silver were obtained when samples were analysed by EDX in one point of the zeolite or by ICP, which is a bulk analysis technique. This is an indication of homogeneous distribution of the silver in the zeolite matrix. This was additionally supported by EDX mapping studies performed in different points of the zeolite, which showed a regular silver distribution in the zeolite. The analyses showed that the Si/Al ratio of the silver-exchanged zeolites was similar to the Si/Al ratio of the parent zeolites, demonstrating that no extraction of aluminium occurred during the ion exchange process. On the other hand, as the

sodium ions were exchanged by silver ions, the amount of sodium in the zeolites decreased as the silver content increased (Table 1).

X-ray diffraction (XRD) measurements were used to evaluate possible modifications in the zeolite structure during the ion exchange process. The diffractogram of the parent Na-FAU zeolite (Fig.1 right) showed the corresponding main peaks assigned to this zeolite at 2θ = 6.23º, 10.10º, 11.85º, 15.67º, 20.37º, 23.65º, 27.03º and 31.38º. Similarly, the parent Na-LTA zeolite (Fig.1 left) showed the peaks characteristic of this zeolite at 2θ = 7.22º, 10.21º, 12.50º, 21.71º, 24.04º, 27.16º, 29.99º and 34.42º. These XRD patterns clearly demonstrated that both parent zeolites had a high crystallinity and absence of amorphous phases. After the silver ion exchange, the peaks appeared at the same positions, evidencing that the ion exchange method carried out to obtain the Ag-zeolites did not produce structural changes in the material and new phases were not formed. However, the intensity of the peaks in the Ag-zeolites varied depending on the level of silver ion exchange. In general, a higher amount of silver in the zeolite resulted in lower peak intensities, but also changes in the relative intensity of the peaks appeared depending on silver content. This behaviour has been also reported with zeolites incorporating silver and others cations [9-11, 29, 30]. As it has been previously described [9], we observed in the Ag-FAU zeolite a clear decrease in the intensity of the peaks at 2θ = 10.10º, 11.85º and 15.67º corresponding to the (220), (311) and (331) reflections if compared with the parent zeolite. This has been related to the redistribution of intra zeolite charge balancing cations [31] or/and with the loss of some crystallinity in the structure [32]. Probably, the changes in the nature, location and amount of extra-framework exchanged species [9, 31] explain the variations in the intensity of the peaks observed in both (LTA and FAU) zeolites after the substitution of Na^+ by Ag^+. On the other hand, no peaks related to metallic silver or to Ag_2O appeared in every silver exchanged zeolite, evidencing that silver was in the ionic form and highly dispersed in the zeolite host.

The morphology of the zeolites after silver exchange was studied by SEM. The micrographies obtained for different Ag-LTA zeolites are shown in Fig. 2. It can be observed that morphology and particle size of both zeolites were similar, consisting of cubic particles from 1.3 to 4.2 μm and they were also analogous to those of the parent zeolite [29]. These results demonstrate that the ion exchange method did not modify the morphology of the zeolite, independently of the amount of exchanged silver. Similar results have been previously reported with FAU samples [25].

In order to analyse the characteristics of the silver species present in the zeolite, H_2-TPR measurements were performed in completely ion exchanged Ag-zeolites. It was initially expected that the present silver species were only Ag^+ since the parent zeolites contain Na^+ cations that have

been exchanged with a silver (I) salt. In contrast, as illustrated in Fig. 3, different profiles were obtained depending on the zeolite. For the Ag-LTA, two peaks appeared at low temperatures around 100 and 140 ºC, being the last one the most significant. Another small and undefined peak was observed at 350 ºC. The attribution of these peaks to particular silver species is not easy as not many previous works have analysed the TPR of this Ag-zeolite. Using other zeolites, some authors [10, 33-35] have assigned the peaks at 100 ºC and 140ºC to large sized AgO and Ag_2O clusters located outside the zeolite, whilst the peak around 350ºC has been assigned to small sized Ag_2O clusters existing inside the zeolite. Other authors [36, 37] assigned the peaks at low temperatures to the reduction of Ag^+, located in different sites of the zeolite and having diverse interactions with the zeolite framework, to Ag_m^{n+} clusters; whilst the peak at higher temperature was assigned to the reduction of the Ag_m^{n+} clusters to Ag_m and/or Ag^0. As Ag_2O and AgO were not observed by XRD, we attributed the main peak at 140 ºC to the reduction of well-dispersed silver oxides (below XRD detection limit) within the pore or on the surface of the zeolite [38], and the peak at 100 ºC to the reduction of Ag^+ exchanged in different sites of the zeolite framework to Ag_m^{n+} clusters that are reduced to Ag_m and/or Ag^0 at 350 ºC. On the other hand, for the Ag-FAU sample, two principal peaks appeared around 100 and 350 ºC and some shoulders were observed at higher temperatures (around 550 and 650 ºC). The peak at 100 ºC can be also attributed to the reduction of Ag^+ to Ag_m^{n+} clusters and the peak at 350 ºC to its reduction to Ag_m and/or Ag^0 or even to successive reduction steps, implying stable Ag_m^{n+} clusters [9, 31, 35]. The shoulders at higher temperature were attributed to isolated Ag^+ ions [38]. It can be expected that as this zeolite has larger cavities and pores than LTA, the formation of silver clusters is more feasible in FAU than in LTA zeolites and for this reason the area of these peaks was larger for FAU zeolites. Nevertheless, additional experiments would be necessary to confirm this hypothesis. In any case, TPR characterization showed the presence of different silver species in the zeolite and/or different location of silver inside the zeolitic structures depending on the zeolite topology.

3.2. Antifungal activity

Preliminary screening of the antifungal properties of silver zeolites was performed by placing directly in the fruit rind wound a drop of aqueous suspension containing 2, 4 or 8% wt of silver completely exchanged LTA zeolite. It was observed that Ag-LTA (te) material was very active and green mold incidence and severity were reduced by 65-85% when compared to control samples (Fig. 4). Maximum activity was obtained with 4 or 8% wt Ag-LTA zeolite, while lower disease reductions were observed with lower silver zeolite content. Therefore, a silver zeolite content of 4% was selected to compare the antifungal activity of different types of Ag-zeolites.

Results obtained with two different Ag-zeolites with different topologies are shown in Fig. 5. The antifungal properties of Ag-LTA zeolite and Ag-FAU-zeolite, both with a complete silver exchange, were studied. Although both zeolites considerably reduced the incidence of the disease, higher reductions were obtained with the Ag-FAU zeolite. The antifungal properties of the parent zeolites (without silver) were also studied and no activity was observed, indicating that the biocide properties of the material were related to the silver released from the zeolite matrix. Silver species locally prevented fungal growth in the inoculation site of the pathogen, but the mechanism of the silver biocide action is not clear. Some researchers proposed that the positive charge of silver ions is responsible for this activity [10, 27]. Fungi are organisms with eukaryotic cells and the electrostatic attraction between the negatively charged cell membrane and the Ag^+ may affect the permeability of the membrane or may allow the transfer of Ag^+ into the cells, damaging the intracellular material. The ion exchange properties of the zeolites facilitate the release of silver cations and the exchange with other ions present in the media, which allows the interaction of released Ag^+ with the cell, disrupting its biochemical activity and causing its death [11]. Moreover, the different silver species observed could have different interactions with fungal cells and different modes of action. For example, in the case of bacteria, it has been proposed that silver ions have affinity for the S-groups of the cell walls resulting in S-Ag bonds that inhibit the H_2 transfer [39]. A similar mechanism could also occur in the case of fungal cells, although it has been repeatedly reported that fungi are more resistant to silver than bacteria [9, 10, 27, 40].

About the different results obtained with Ag-FAU and Ag-LTA, the best antifungal activity was observed with the Ag-FAU zeolite, even though this zeolite contained a lower percentage of silver due to its lower aluminium content. These results must be related to the different Si/Al ratio of the zeolites or to their different topologies and probably both characteristics affect the antifungal activity of the materials. Since the mechanism for cell death needs the contact of the silver with the cell wall, it could be expected that the topology of the zeolites has an important influence on their antifungal properties. FAU zeolite is a three-dimensional zeolite with super-cages and pores of 7.4 x 7.4Å (large pore size) while LTA is a three-dimensional zeolite with super-cages and pores of 4.1 x 4.1Å (small pore size). Thus, FAU zeolite, which has larger pore sizes than LTA zeolite, provided a better release of Ag^+ to the media and an enhanced contact of Ag^+ with the fungal cells, resulting in higher fungicidal activity. In addition, it has been described [9] that in this zeolite, silver is present mainly in the ionic form, whilst in zeolites with lower Si/Al ratio, metallic silver is more easily formed. As the antifungal agent is the cationic form of silver (Ag^+), FAU-zeolites are expected to be more active than Ag-LTA. TPR experiments confirmed these hypotheses and, as illustrated in Fig.

3, the silver species present in the Ag-LTA zeolite were more easily reducible than those present in the Ag-FAU zeolite, indicating that metallic silver can be likely formed in the former zeolite.

Nevertheless, it was observed that in spite of the antifungal properties of these materials they caused an apparent fruit phytotoxicity, appearing circular black spots surrounding the rind wound (Fig. 6). According to Quah *et al.* [41], among different silver species, Ag^+ at the same nominal concentration displays the strongest potential to induce phytotoxicity in plants due to its physical and chemical properties at high concentration. For this reason, additional in vivo tests with reduced amounts of silver in the zeolites (partial exchange, around 1-2% wt) were conducted in an attempt to overcome these problems. In this case, the silver zeolites were incorporated into composite HPMC-BW edible coatings, which were applied to the fruit as either drops in the inoculation site (orange rind wound) or manual coating of the entire fruit. As shown in Fig. 7, decreasing the silver content in both zeolites resulted in a decrease of the antifungal activity when the antifungal coating was applied as a drop. Nevertheless, it must be pointed out that a reduction of twenty-five times of the silver content in the zeolites only resulted in a half reduction of the Ag-LTA antifungal activity, and even less for the Ag-FAU. Experiments made with the latter showed that the application of this zeolite with 1.3% wt of silver, reduced green mold incidence and severity by 55 and 72%, respectively. As it has been previously discussed, these results can be explained by the different pore size of the zeolites. FAU zeolite with a higher pore size than LTA zeolite facilitates the release of ionic silver and its interaction with fungal structures. Furthermore, the FAU zeolite used in this study had a Si/Al ratio of 2.4 while the LTA zeolite had a Si/Al ratio of 1. As the level of silver exchange depends on the aluminium content, even a lower percentage of silver in the zeolite with the highest Si/Al ratio results in a higher level of exchanged positions (see Table 1). This may produce a better dispersion of Ag^+ in the zeolite framework, allowing a better contact of the released cations with fungal cells and consequently, improving its antifungal properties. Then, the larger pores and the higher Si/Al ratio of the Ag-FAU zeolite may explain the best fungicidal activity of this material if compared with that of the Ag- LTA. Nevertheless, the effect of the presence of different type of silver species with different antifungal activity in both zeolites should not be excluded. As it was concluded from the TPR experiments, it seems that Ag-FAU presented more different silver species than Ag-LTA and it has been described [10] that the diversification of silver species favours the biocide activity of the zeolites due to different diffusion rates and different interactions with microbial cells.

Finally, a commercial application of edible coatings containing Ag-zeolite was resembled in in vivo trials. Oranges previously inoculated with *P. digitatum* were coated by uniformly distributing the coating over the entire fruit surface and the reduction of the incidence and severity of green

mold was compared to those obtained by applying the coating as a drop in the pathogen inoculation site. Results showed that drop application in the wound resulted more effective than complete fruit coating application, which could be attributed to a better coverage of the infection site and an easier interaction of the silver with fungal cells. In addition, it was observed that the application of HPMC-BW coating containing Ag-FAU zeolite with 1.3% wt of silver did not induce any type of apparent phytotoxicity in the orange rind due to the low silver content in the formulation.

4. Conclusions

Results show the potential of silver zeolites as active antifungal materials for the control of important postharvest diseases of fresh horticultural produce such as the citrus green mold caused by *P. digitatum*. The incorporation of these zeolites into edible coatings also significantly controlled decay of oranges. The antifungal activity of the silver zeolites depended on the amount of silver, the Si/Al ratio and the topology of the zeolites. In general, higher silver content resulted in better antifungal activity but caused apparent phytotoxicity on the fruit surface. Nevertheless, Ag-zeolites with a low silver content were also effective without producing phytotoxic effects. The best results were obtained with the zeolite with the largest pores and the highest Si/Al ratio. Both characteristics facilitated the release of the Ag^+ antifungal agent and its contact with fungal cells. Characterization studies have shown that the silver exchange process did not modify the zeolite structure and that silver was mainly present as well dispersed Ag^+. Nevertheless, the silver species and the interaction with the zeolite structure depended on the zeolite topology and might result in different antifungal properties. In this study the best results were obtained with the Ag-FAU.

Acknowledgements

The authors thank the Spanish Ministry of Economy and Competitiveness and the Fondo Europeo de Desarrollo Regional through MAT2015-71842-P (MINECO/FEDER) for the financial support. J.L. Cerrillo wishes to thank MINECO for the Severo Ochoa contract for PhD formation (SVP-2014-068600).

REFERENCES

[1] J. Gustavsson, C. Cederberg, U. Sonneson, R. Van Otterdijk and A. Meybeck, Perdidas y desperdicio de alimentos en el mundo: Alcance, causa y prevencion, FAO, Roma (Italia). Swedish Institute for Food and Biotecnology Gothenburg (Suecia).2012.

[2] M. B. Pérez-Gago, Palou, L. , Antimicrobial packaging for fresh and fresh-cut fruits and vegetables. In: Fresh-Cut Fruits and Vegetables: Technology, Physiology, and Safety, in: S. Pareek (Ed.), CRC Press, Taylor and Francis Group, Boca Raton, FL, USA, 2016, pp. 403-452

[3] L. Palou, Smilanick, J.L., Montesinos-Herrero, C., Valencia-Chamorro, S., Pérez-Gago, M.B. , Novel approaches for postharvest preservation of fresh citrus fruits. In: Citrus Fruits: Properties, Consumption and Nutrition, D.A. Nova Science Publishers, Inc, New York (U.S.A.), 2011.

[4] P. Lalueza, M. Monzon, M. Arruebo and J. Santamaria, Mater. Res. Bull., 46 (2011) 2070-2076.

[5] P. Saint-Cricq, Y. Kamimura, K. Itabashi, A. Sugawara-Narutaki, A. Shimojima and T. Okubo, Eur. J. Inorg. Chem., 2012 (2012) 3398-3402, S3398/1-S3398/2.

[6] C. Costa, A. Conte, G. G. Buonocore and M. A. Del Nobile, Int. J. Food Microbiol., 148 (2011) 164-167.

[7] T. Jiang, L. Feng and Y. Wang, Food Chem., 141 (2013) 954-960.

[8] X. Chen and H. J. Schluesener, Toxicol. Lett., 176 (2008) 1-12.

[9] L. Ferreira, A. M. Fonseca, G. Botelho, C. Almeida-Aguiar and I. C. Neves, Microporous Mesoporous Mater., 160 (2012) 126-132.

[10] C. Chiericatti, J. C. Basilico, M. L. Z. Basilico and J. M. Zamaro, Microporous Mesoporous Mater., 188 (2014) 118-125.

[11] A. M. Pereyra, M. R. Gonzalez, V. G. Rosato and E. I. Basaldella, Prog. Org. Coat., 77 (2014) 213-218.

[12] US FDA, 2007. Inventory of Effective Food Contact Substance (FCS) Notifications: Zeolite A in which silver and zinc ions have been exchanged for sodium ions, FCS No. 697. U.S. Food and Drug Administration, Washington, D.C.

[13] M. Corrales, A. Fernández and J.J. Han, (2014). Antimicrobial packaging systems. In: Innovations in food packaging, 2nd ed., Han, J.H., (Ed.), Academic Press, Waltham, MA, pp. 133-170.

[12] Y. Matsumura, K. Yoshikata, S.-i. Kunisaki and T. Tsuchido, Appl. Environ. Microbiol., 69 (2003) 4278-4281.

[13] J. Hrenovic, J. Milenkovic, I. Goic-Barisic and N. Rajic, Microporous Mesoporous Mater., 169 (2013) 148-152.

[14] Y. Inoue, M. Hoshino, H. Takahashi, T. Noguchi, T. Murata, Y. Kanzaki, H. Hamashima and M. Sasatsu, J. Inorg. Biochem., 92 (2002) 37-42.

[15] K. K. Krishnani, Y. Zhang, L. Xiong, Y. Yan, R. Boopathy and A. Mulchandani, Bioresour. Technol., 117 (2012) 86-91.

[16] T. Matsumura, Y. Abe, Y. Sato, K. Okamoto, M. Ueshige and Y. Akagawa, J. Dent., 25 (1997) 373-377.

[17] N. S. Flores-Lopez, J. Castro-Rosas, R. Ramirez-Bon, A. Mendoza-Cordova, E. Larios-Rodriguez and M. Flores-Acosta, J. Mol. Struct., 1028 (2012) 110-115.

[18] A. Top and S. Ulku, Appl. Clay Sci., 27 (2004) 13-19.

[19] S. M. Magana, P. Quintana, D. H. Aguilar, J. A. Toledo, C. Angeles-Chavez, M. A. Cortes, L. Leon, Y. Freile-Pelegrin, T. Lopez and R. M. Torres Sanchez, J. Mol. Catal. A Chem., 281 (2008) 192-199.

[20] I. De la Rosa-Gomez, M. T. Olguin and D. Alcantara, J. Environ. Manage., 88 (2008) 853-863.

[21] K. Kawahara, K. Tsuruda, M. Morishita and M. Uchida, Dent. Mater., 16 (2000) 452-455.

[22] T. Haile and G. Nakhla, Biodegradation, 21 (2010) 123-134.

[23] H. Nikawa, T. Yamamoto, T. Hamada, M. B. Rahardjo, H. Murata and S. Nakanoda, J. Oral Rehabil., 24 (1997) 350-357.

[24] K. Malachova, P. Praus, Z. Rybkova and O. Kozak, Appl. Clay Sci., 53 (2011) 642-645.

[25] B. Kwakye-Awuah, C. Williams, M. A. Kenward and I. Radecka, J. Appl. Microbiol., 104 (2008) 1516-1524.

[26] P. Lalueza, M. Monzon, M. Arruebo and J. Santamaria, Chem. Commun. (Cambridge, U. K.), 47 (2011) 680-682.

[27] R. S. Bedi, R. Cai, C. O'Neill, D. E. Beving, S. Foster, S. Guthrie, W. Chen and Y. Yan, Microporous Mesoporous Mater., 151 (2012) 352-357.

[28] S. A. Valencia-Chamorro, L. Palou, M. A. del Río and M. B. Pérez-Gago, Critical Reviews in Food Science and Nutrition, 51 (2011) 872-900.

[29] A. Mayoral, T. Carey, P. A. Anderson and I. Diaz, Microporous Mesoporous Mater., 166 (2013) 117-122.

[30] S. A. Valencia-Chamorro, Ll. Palou, M. A. del Río, M. B. Pérez-Gago, J. Agric. Food Chem., 56 (2008) 11270-11278.

[30] S. Demirci, Z. Ustaoglu, G. A. Yilmazer, F. Sahin and N. Bac, Appl. Biochem. Biotechnol., 172 (2014) 1652-1662.

[31] M. Salavati-Niasari, Polyhedron, 28 (2009) 2321-2328.

[32] D. L. Boschetto, L. Lerin, R. Cansian, S. B. C. Pergher and M. Di Luccio, Chem. Eng. J. (Amsterdam, Neth.), 204-206 (2012) 210-216.

[33] T. Furusawa, K. Seshan, J. A. Lercher, L. Lefferts and K.-i. Aika, Appl. Catal., B, 37 (2002) 205-216.

[34] K. A. Bethke and H. H. Kung, J. Catal., 172 (1997) 93-102.

[35] E. Sayah, D. Brouri and P. Massiani, Catal. Today, 218-219 (2013) 10-17.

[36] J. Shibata, K.-i. Shimizu, Y. Takada, A. Shichi, H. Yoshida, S. Satokawa, A. Satsuma and T. Hattori, J. Catal., 227 (2004) 367-374.

[37] R. Bartolomeu, B. Azambre, A. Westermann, A. Fernandes, R. Bertolo, H. I. Hamoud, C. Henriques, P. Da Costa and F. Ribeiro, Appl. Catal., B, 150-151 (2014) 204-217.

[38] D. Chen, Z.-P. Qu, S.-J. Shen, X.-Y. Li, Y. Shi, Y. Wang, Q. Fu and J.-J. Wu, Catal. Today, 175 (2011) 338-345.

[39] R. L. Davies and S. F. Etris, Catal. Today, 36 (1997) 107-114.

[40] A.D. Russell, W.B. Hugo and G. A. J. Ayliffe, Desinfectation, Preservation and Sterilization, Blackwell Scientific Publications, Oxford, UK, 1992.

[41] B. Quah, C. Musante, J. C. White and X. Ma, J. Nanopart. Res., 17 (2015) 1-13.

Table 1

Chemical composition of the zeolites measured by ICP-OES (a) or by EDX (b).

	wt% Ag[a]	Si/Al molar ratio[a]	% ion exchange[a]	wt% Ag[b]	wt% Na[b]	Si/Al molar ratio[b]
LTA	-	1.0	-	-	16.2	1.0
LTA_Ag(te)	48.4	0.9	95.9	49.1	0.5	1.1
LTA_Ag(pe)	1.8	0.9	2.7	1.9	13.9	1.0
FAU	-	2.4	-	-	4.8	2.6
FAU_Ag(te)	30.6	2.5	93.4	-	-	-
FAU_Ag(pe)	1.3	2.4	3.4	-	-	-

Caption to figures

Figure 1. XRD patterns of LTA (left) and FAU (right) zeolites in the sodium form (a), partially silver ion-exchanged (b) and with a complete silver ion-exchange (c).

Figure 2. SEM images of Ag-LTA zeolites with low silver content (partial exchange, pe) and with a complete silver ion exchange (total exchange, te).

Figure 3. TPR profiles of Ag-LTA zeolite (a) and Ag-FAU (b) with a complete silver ion exchange (total exchange, te).

Figure 4. Curative activity against green mold on 'Valencia' oranges inoculated in a rind wound with *P. digitatum*, treated with LTA_Ag(te) at different concentrations and incubated for 7 days at 20 ºC. Zeolite was applied in aqueous suspension as a drop in the wound. Vertical lines in columns describe standard error.

Figure 5. Curative activity against green mold on 'Valencia' oranges inoculated in a rind wound with *P. digitatum*, treated with different Ag-zeolites and incubated for 7 days at 20 ºC. Zeolite was applied at 4% in aqueous suspension as a drop in the wound.

Figure 6. Photographs of Valencia' oranges inoculated, treated and incubated at 20 ºC for 7 days: non-treated control samples (1), oranges treated with LTA_Ag(te) (2) and oranges treated with FAU_Ag(te) (3). Detail of the phytotoxicity induced by the Ag-zeolite (4).

Figure 7. Curative activity against green mold on 'Valencia' oranges inoculated in a rind wound with *P. digitatum*, treated with HPMC-BW edible coatings containing Ag-zeolites with low silver content (partial exchange, pe) and incubated for 7 days at 20 ºC. Coatings were applied as a drop in the wound. Vertical lines in columns describe standard error.

Figure 8. Comparison of curative activity against green mold on 'Valencia' oranges inoculated in a rind wound with *P. digitatum*, treated with HPMC-BW edible coatings containing FAU_Ag(pe) and incubated for 7 days at 20 ºC. Coatings were applied as a as a coating over the complete orange rind (left) or as a drop in the wound (right). Vertical lines in columns describe standard error.

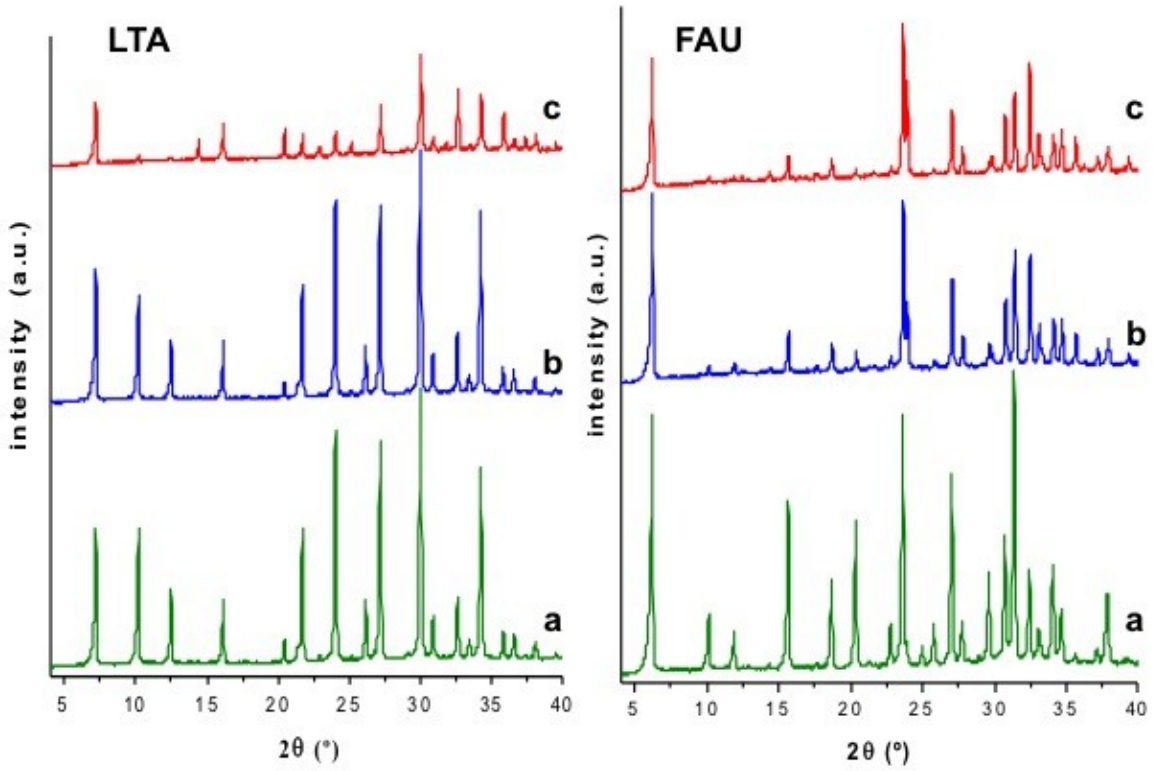
LTA
FAU
intensity (a.u.)
intensity (a.u.)
c
b
a
c
b
a
5
10
15
20
25
30
35
40
2θ (°)
2θ (°)

Fig,. 1

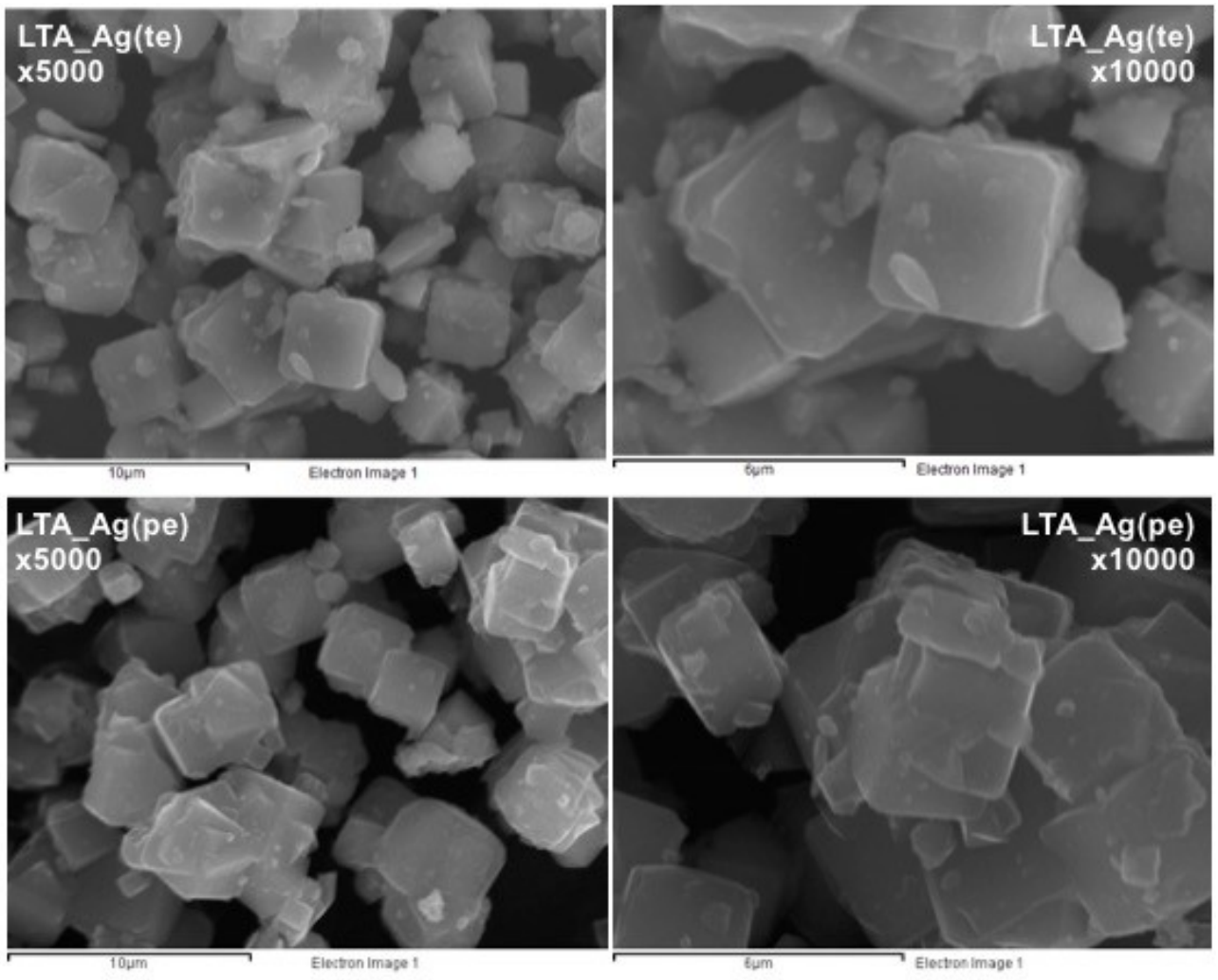
LTA_Ag(te)
x5000
10µm
Electron Image 1
LTA_Ag(te)
x10000
5µm
Electron Image 1
LTA_Ag(pe)
x5000
10µm
Electron Image 1
LTA_Ag(pe)
x10000
5µm
Electron Image 1

Fig. 2

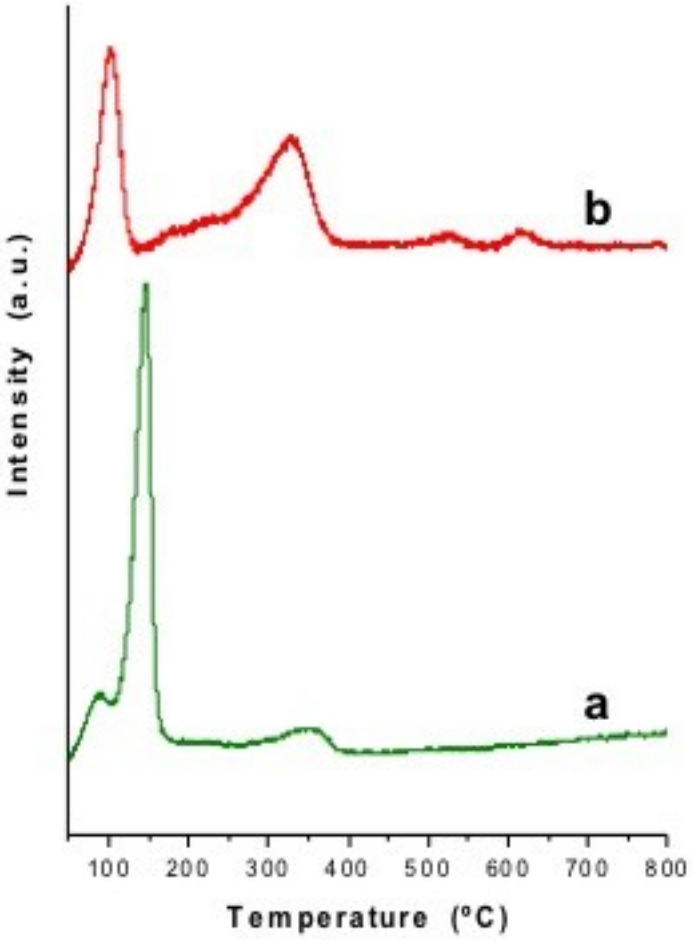

Fig. 3

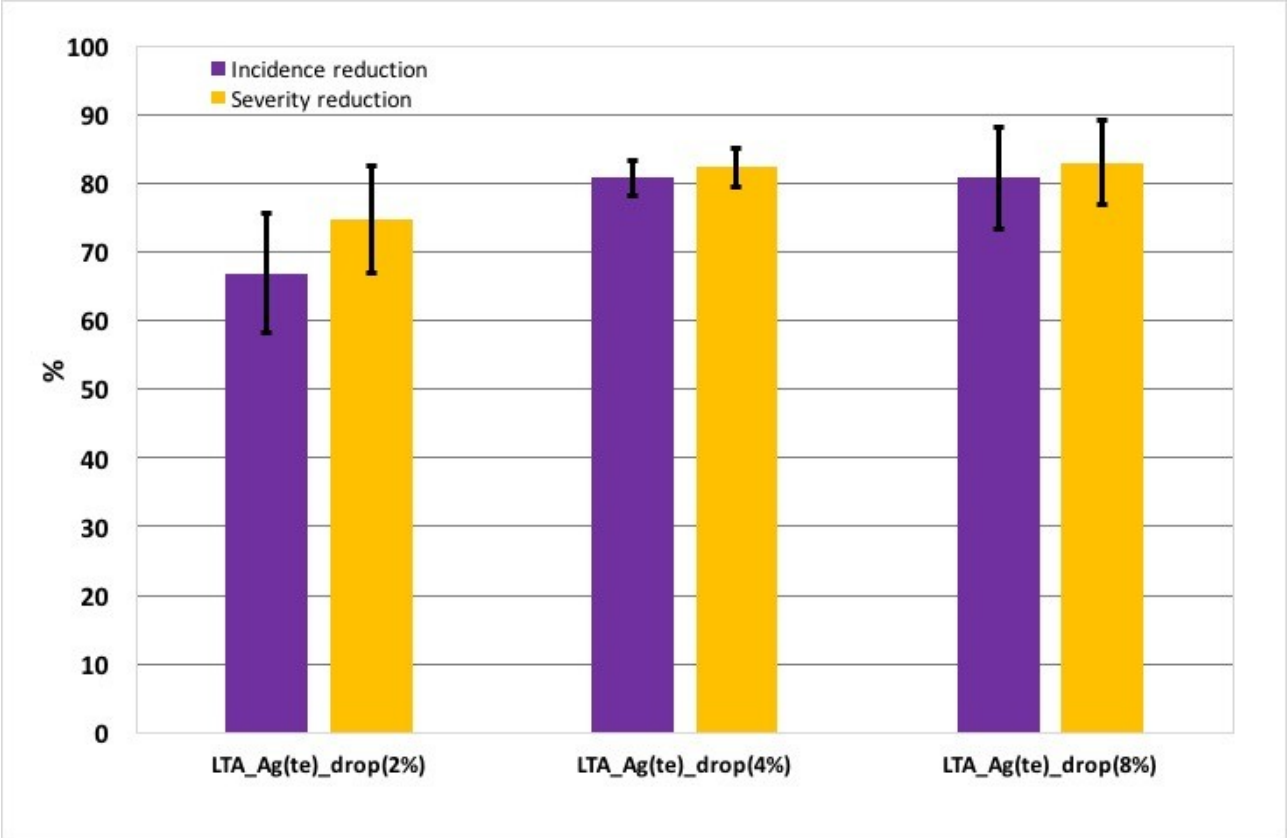
100
90
80
70
60
50
40
30
20
10
0
%
Incidence reduction
Severity reduction
LTA_Ag(te)_drop(2%)
LTA_Ag(te)_drop(4%)
LTA_Ag(te)_drop(8%)

Fig. 4

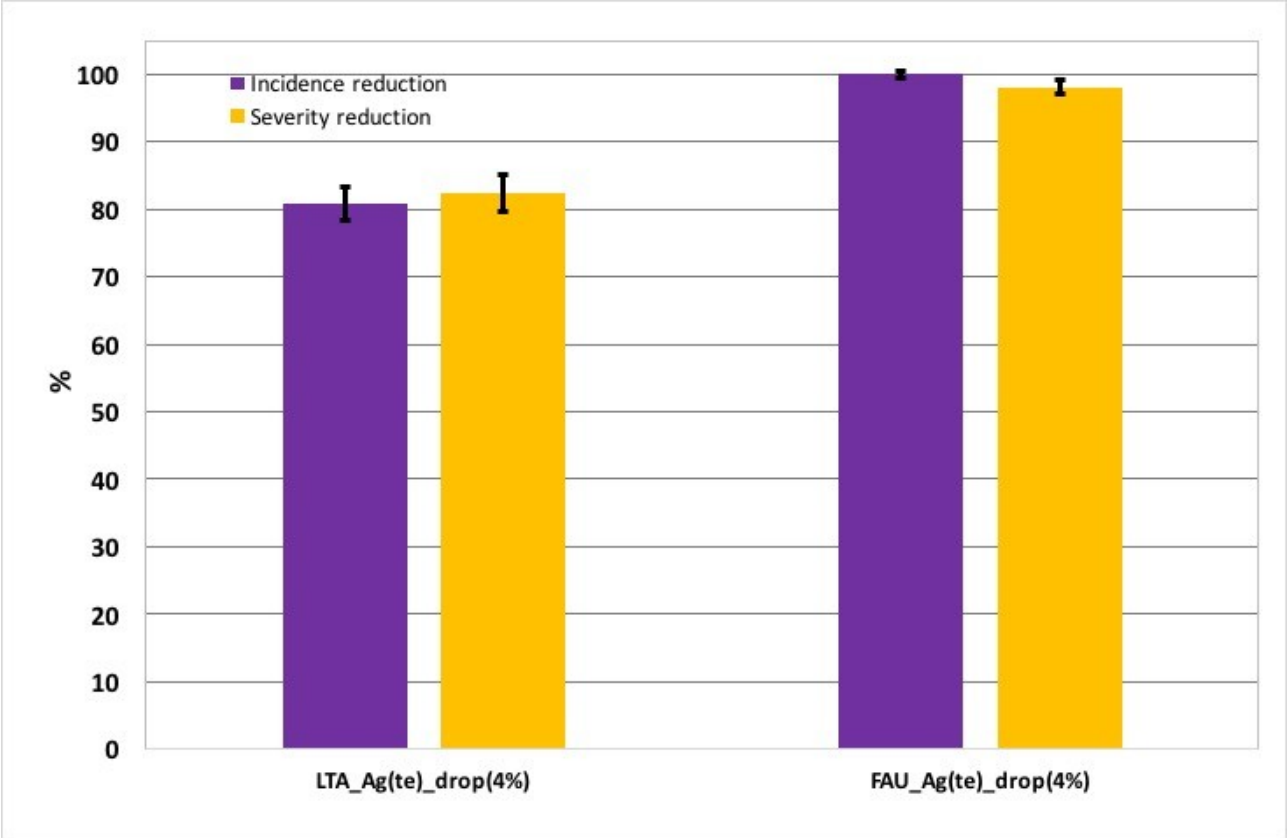
Incidence reduction
Severity reduction
100
90
80
70
60
50
40
30
20
10
0
%
LTA_Ag(te)_drop(4%)
FAU_Ag(te)_drop(4%)

Fig. 5

Fig. 6

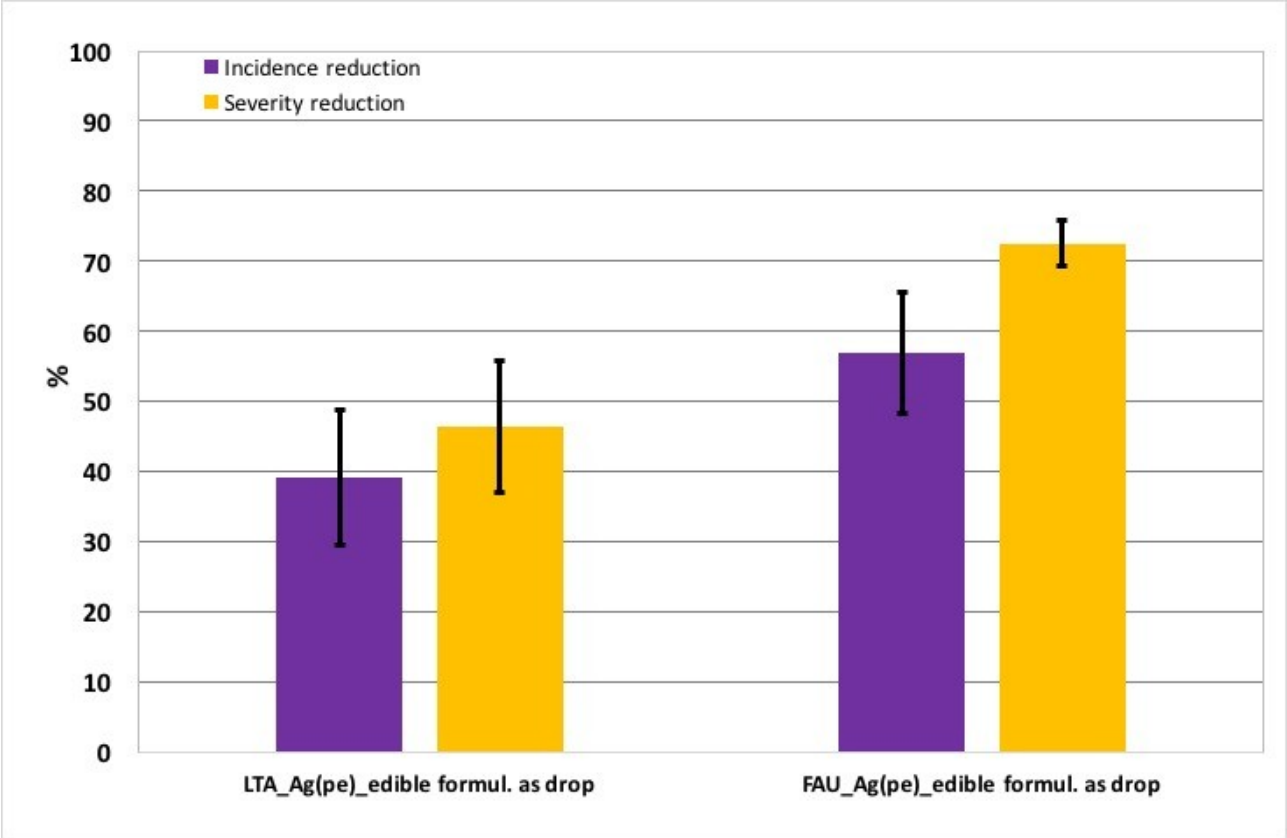
Incidence reduction
Severity reduction
100
90
80
70
60
50
40
30
20
10
0
%
LTA_Ag(pe)_edible formul. as drop
FAU_Ag(pe)_edible formul. as drop

Fig. 7

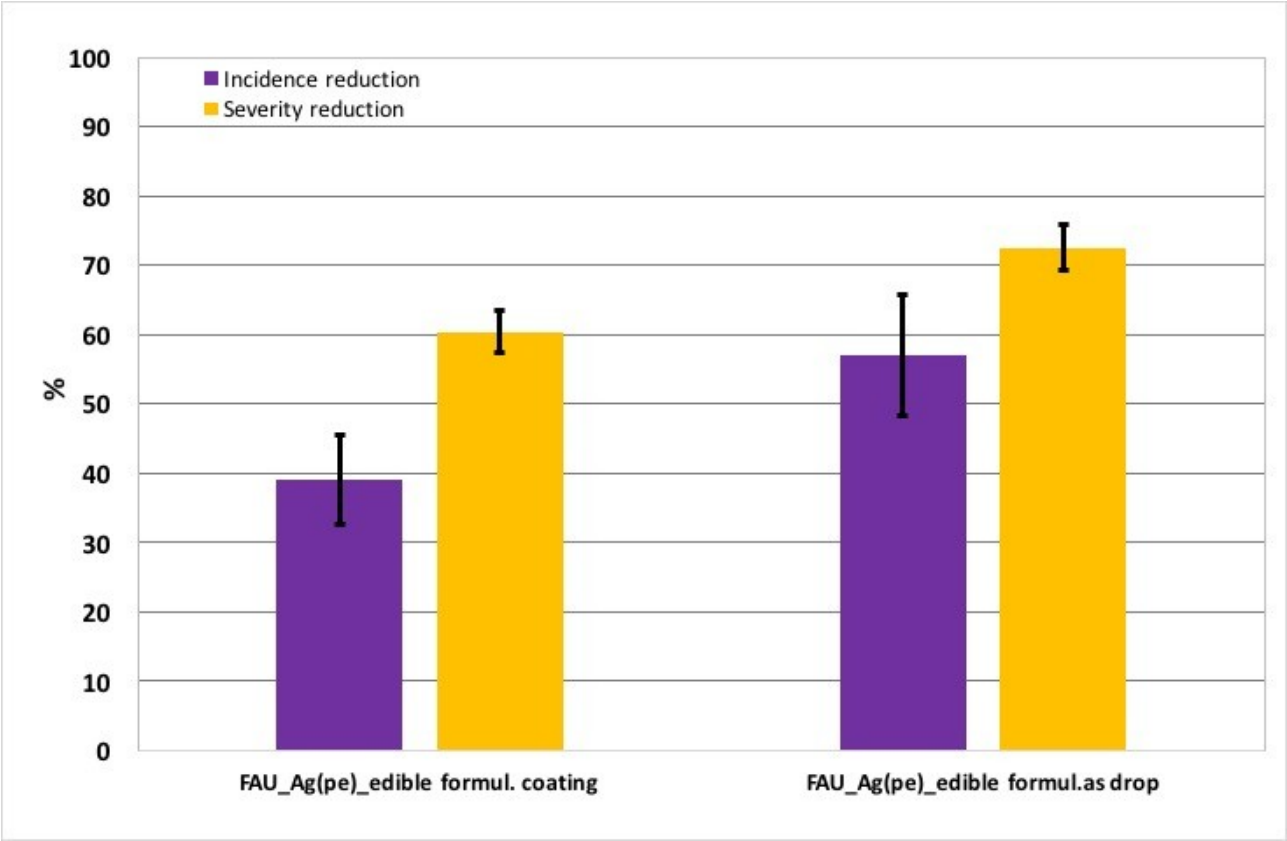
100
90
80
70
60
50
40
30
20
10
0
%
Incidence reduction
Severity reduction
FAU_Ag(pe)_edible formul. coating
FAU_Ag(pe)_edible formul.as drop

Fig. 8